



Analysis of coastal changes using remote sensing and geographical information systems in the Gulf of Izmit, Turkey

Dilara Ciritci · Tarık Türk 

Received: 14 November 2019 / Accepted: 27 March 2020 / Published online: 8 May 2020
© Springer Nature Switzerland AG 2020

Abstract The shoreline is constantly under the influence of physical elements, such as geomorphological events, earthquakes, and tectonic movements. In recent years, it has been changing due to the intensive use of coasts and the impact of human factors on coastal areas. This study's aim was to analyze the coastal change in the Gulf of Izmit, Turkey, using satellite images from different dates. In this context, coastal changes were analyzed in a 95% confidence interval by the end point rate (EPR), linear regression rate (LRR), and weighted linear regression (WLR) statistical methods, after the automatic extraction of shorelines from Landsat satellite images of 17 periods belonging to different dates between 1975 and 2017 in four different scenarios. Furthermore, the effects of the destructive earthquake (Mw, 7.4), which caused the loss of many lives and property in the Gulf of Izmit on August 17, 1999, were also examined in detail.

Keywords GIS · Coastline · Change detection · Digital shoreline analysis system

Introduction

Coasts are important areas located at the intersection point of marine and terrestrial natural areas in which

people have been interested from past to present and where they benefit from all kinds of activities. In the world, factors, such as intensive population growth, industrialization, transportation, and tourism, and the opportunities offered by the coast have exposed coasts to excessive use (Uzun and Garipağaoğlu 2014). This excessive use can disrupt the delicate balance of the coastal ecosystem. These areas are areas where, besides human-centered pressures, deterioration of natural processes is also effective. Therefore, the ecological sustainability of these areas is essential (Tağıl and Cürebal 2005).

Gibeaut et al. (2001) divided changes in the shoreline into three: long-term change, short-term change, and episodic shoreline retreat. In this context, long-term changes describe changes that occur between 10 and 1000 years, while short-term changes cover only changes that take place between 5 and 10 years. Episodic shoreline retreat is defined as sudden changes caused by natural events, such as floods and storms. While long-term changes affect the whole coast at the same level, regression in short-term changes is observed on one side on the same coast at intervals of several kilometers. In contrast, on the other side, it can be observed that the land is progressing or is stationary. Due to natural characteristics of low coasts, these changes occur in the form of regression or transgression as a result of alterations in natural conditions, such as waves and winds (Kalkan et al. 2010). Nowadays, there are many studies in the literature on determining shoreline changes occurring in coastal regions, estimating the future position of the shoreline, and examining factors that cause the shoreline change. The digital shoreline

D. Ciritci · T. Türk (✉)
Department of Geomatics Engineering, Sivas Cumhuriyet
University, Faculty of Engineering, 58140 Sivas, Turkey
e-mail: tarikturk@gmail.com

analysis system (DSAS) is one of the most widely used methods for the analysis of these studies in the world.

Beyazıt (2014) examined shoreline changes that occurred in the Kızılırmak Delta between 1987 and 2011. The researcher used the band rating technique for the determination of shorelines and the shoreline change envelope (SCE), end point rate (EPR), and linear regression rate (LRR) analysis methods included in DSAS for the determination of shoreline changes. As a result of the analysis, he detected a displacement in the direction of the land, of which maximum value was 655.6 m with the erosion amount of around -27.38 m/year between 1987 and 2011 in the Kızılırmak Delta shoreline. Kuleli et al. (2011) performed the coastal change analysis in Turkey's Ramsar wetlands by using DSAS and Landsat satellite images. Five different wetlands were selected for the analysis: Yumurtalık Ramsar, Göksu Ramsar, Kızılırmak wetland, Yeşilirmak wetland, and Gediz wetland. As a result of the analysis, significant shoreline changes were observed in some parts of the study area during three periods (1989, 1999, and 2009). During the period between 1975 and 2009, the 35.57 km² wetland in the Gediz Delta turned into the sea or salt marsh. Güneroğlu (2015) examined morphological changes that occurred in the coastal area of Trabzon (Turkey) in 4 different periods between 1984 and 2011. The researcher benefited from Landsat satellite images for the determination of shoreline changes and calculated shoreline changes that occurred over 27 years using the DSAS. A total of 897 transects were produced at 100-m intervals in the study area. Each coastal district was analyzed separately, and the relevant statistics were calculated. The researcher preferred the LRR method to minimize the effect of random error and short-term changes (Crowell et al. 1997; Maiti and Bhattacharya 2009). As a result, he detected that the net shoreline change in the center of Trabzon reached 88.2 m and observed that accretion activities occurred along the coast due to anthropogenic effects. Ciritci and Türk (2019) aimed to reveal shoreline changes in the Göksu Delta with Landsat satellite images and GIS-based analyses. They analyzed coastal changes that occurred between 1984 and 2011 (1984, 1998, 2003, 2006, 2011) in a 95% confidence interval with the help of the SCE, EPR, and LRR methods in the DSAS. On the other hand, Uzun (2014) analyzed coastal changes that occurred along the Hersek Delta coasts in the Gulf of İzmit using remote sensing and GIS techniques by the supervised and unsupervised classification of Landsat

satellite images of 2004, 2009, and 2014. As a result, while the shore length in the study area was 17.07 km and land area was 2193 ha in 2004, it was found that the shore length increased to 24.48 km and land area increased to 2388 ha in 2014.

Alberti et al. (2013) analyzed shoreline changes that occurred between the years of 1956, 2003, 2006, and 2008 on the coast of Galicia in Spain using the linear regression rate (LRR), weighted linear regression (WLR), end point rate (EPR), and net shoreline movement (NSM) statistical methods of the DSAS. Addo et al. (2008) used the LRR method in DSAS by benefiting from the maps of 1904, 1974, 1996, and 2002 to analyze the coastal change in the Accra region of Ghana. Arockiaraj et al. (2018) determined the coastal change on the Bhatye and Ganapathypule coasts of the Ratnagiri region located on the western coast of India for the years 2014–2015 using the NSM method in DSAS. Mukhopadhyay et al. (2012) aimed to analyze the shoreline change that occurred in the Puri region of India due to erosion and accretion by using Landsat images belonging to the years 1972, 2001, and 2010 and aimed to predict the future shoreline. The study was conducted on a 142-km shoreline in the Puri region. Based on empirical observations, the researchers used the EPR method to analyze the shoreline and the rate of change in the location of the coast in the future. They detected that the amount of erosion around Kushabhadra in the north of Puri and on the Chandrabhaga coast was high and estimated short-term (2015) and long-term (2025) shoreline locations. Nassar et al. (2019) aimed to detect the coastal change along the North Sinai coast in Egypt with Landsat satellite images using DSAS. To determine shoreline morphodynamics on the Crantock coasts in southwestern England, Oyedotun (2014) analyzed the 124-year coastal change in the study area with maps belonging to the years of 1888 and 2012 by benefiting from the EPR, SCE, and NSM statistics of the DSAS. As a result of the study, they concluded that erosion occurred on the Crantock coasts to a large extent. Sheik and Chandrasekar (2011) studied coastal changes in South India using DSAS. According to geological and hydrological characteristics, they divided the entire study area into four coastal regions and used IRS and Landsat satellite data (1999, 2001, 2003, 2005, 2007, and 2009) to extract the shoreline. As a result of the shoreline change analysis, erosion was observed to be dominant

in the study area. Thang et al. (2017) aimed to determine the shoreline change on the Kien Giang coast of the Mekong River Delta in Vietnam using the DSAS. As a result of the analysis, they detected the erosion amount on the Kien Giang coast to be 4.8 m/year on average and the accretion amount to be 5.7 m/year in the 40 years covering the period between 1973 and 2013. Yunus Ali and Narayana (2015) analyzed the shoreline change that occurred in Trinket Island due to the tsunami disaster that took place in India in 2004, by benefiting from satellite images for the years 2004–2013 and using the EPR, LRR, and NSM methods in the DSAS. As a result of the study, they emphasized that the amount of erosion was more dominant than the amount of accretion, and the shoreline erosion was obtained to be -9 m/year on average.

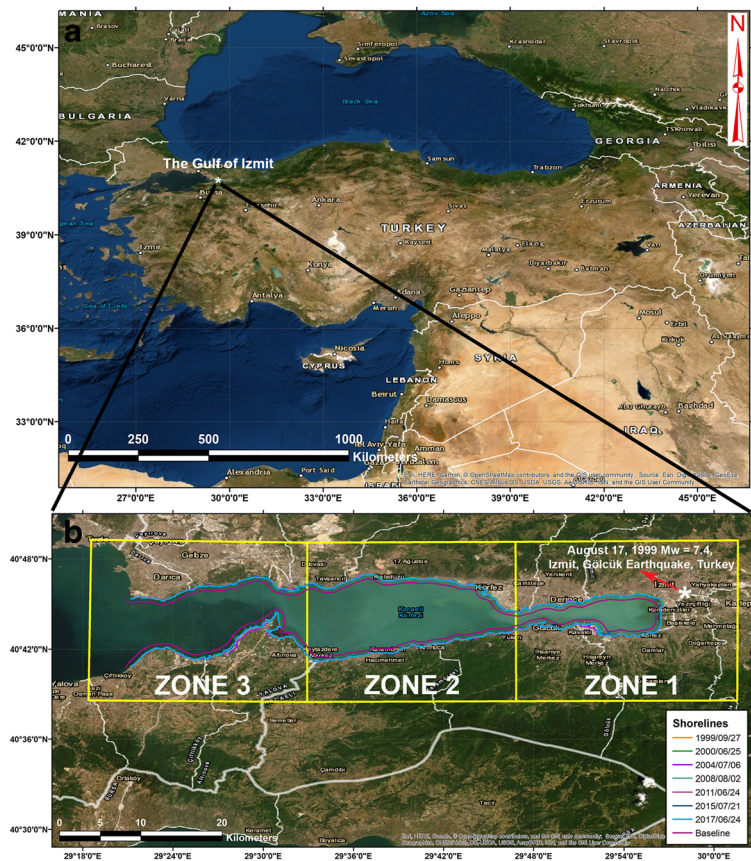
This study’s aim was to investigate the coastal change in the Gulf of Izmit, Turkey. In the study, four different scenarios were used. In this context, after the precise automatic extraction of shorelines from Landsat satellite images of 17 periods belonging to different

dates between 1975 and 2017, coastal changes were analyzed in a 95% confidence interval with the EPR, LRR, and WLR statistical methods. Furthermore, this study reveals the effects of the earthquake on the shoreline by remote sensing and GIS-based analyses before and after the 17 August 1999 earthquake in Gölcük, Turkey (Mw = 7.4).

Study area

The study area covers the coasts of the Gulf of Izmit, Turkey, which is one of the most prominent areas where the coastal use increases depending on the geomorphological structure and as a result of which changes occur (Fig. 1). The Gulf of Izmit is one of the areas, which is found in the east of the Marmara region and has a coastal length of approximately 130 km and where intensive activities take place in terms of coastal use (Uzun 2015). The widest part of the Gulf of Izmit is 9.6 km between Hereke and Karamürsel, and the narrowest parts are

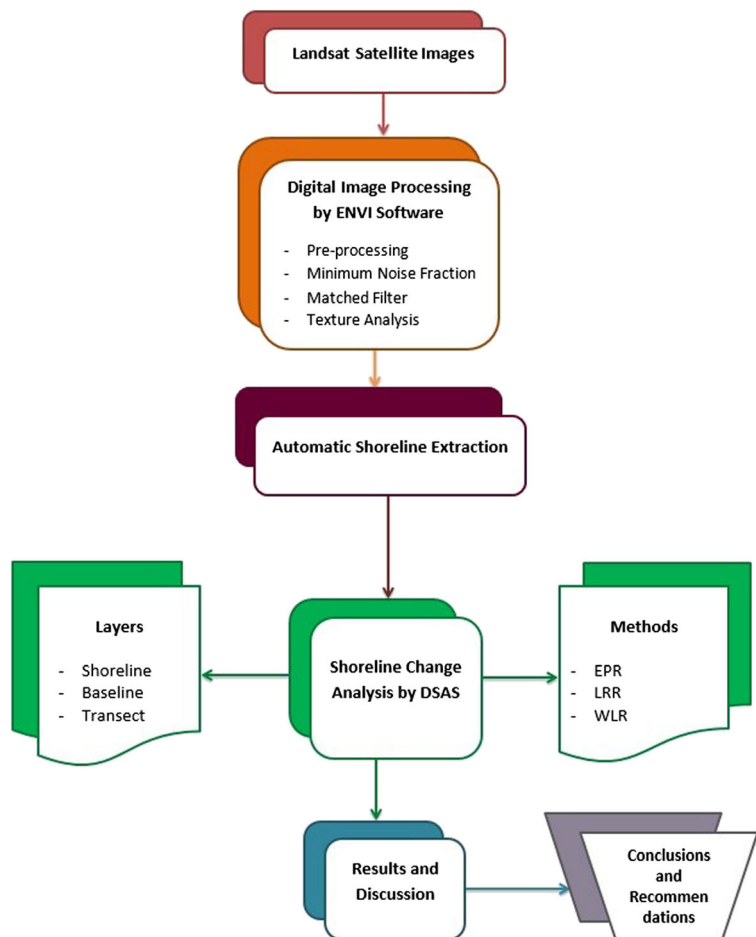
Fig.1 a General view of the study area. b The study area



2.7 km between Dil Burnu and Hersek Burnu and 1.8 km between Derince and Değirmendere (Hoşgören 1995). The alluvial area formed as a result of the accumulation of the materials carried by the rivers in the east of the Gulf of Izmit is of a lowland character (Göney 1963; Hoşgören 1995).

Another important feature of the study area is that it is located on the North Anatolian Fault Zone and is at high risk of an earthquake. The earthquake of 7.4 (Mw) magnitude occurred on 17 August 1999 in the Gulf of Izmit, where industrial centers were present and urbanization and population density were high. Thus, a significant loss of lives and property occurred (Özmen 2000). As a result of this earthquake, the greatest loss of lives and property in Kocaeli province occurred in Gölcük district. Of the houses in Gölcük, 35.7% were severely damaged, and 5239 people living in this district died (Demirtaş 2000).

Fig. 2 Steps followed in the study



Materials and methods

In this study, ENVI 5.3 software was used for the processing of satellite images, the ArcGIS 10.5 software was used for the extraction of shorelines from the processed satellite images, and DSAS 5.0 (Himmelstoss et al. 2018) was used in the coastal change analysis.

The process steps followed in the study are presented in Fig. 2.

Data used

In the study, a total of 17 periods of Landsat satellite images covering 42 years between 1975 and 2017 were used (Table 1). While determining satellite images belonging to different years, attention was paid to the selection of dates close to each other to minimize the effects of seasonal differences on the coast. However, in the selection of the dates of satellite images used in the

Table 1 Satellite images used in the study

Pre-earthquake	Date of image	Satellite image	Sensor	Datum	Projection	Resolution (m)	Path/row	File type	Cloudiness rate
	17.06.1975	Landsat 2	MSS	WGS 84	UTM zone 36 N	60 × 60	193/032	GEOTIFF	0
	10.07.1985	Landsat 5	TM	WGS 84	UTM zone 36 N	30 × 30	179/032	GEOTIFF	0
	23.07.1987	Landsat 5	TM	WGS 84	UTM zone 36 N	30 × 30	180/032	GEOTIFF	1
	03.08.1988	Landsat 5	TM	WGS 84	UTM zone 36 N	30 × 30	179/032	GEOTIFF	6
	06.08.1989	Landsat 5	TM	WGS 84	UTM zone 36 N	30 × 30	179/032	GEOTIFF	0
	27.07.1991	Landsat 5	TM	WGS 84	UTM zone 36 N	30 × 30	179/032	GEOTIFF	0
	06.07.1995	Landsat 5	TM	WGS 84	UTM zone 36 N	30 × 30	179/032	GEOTIFF	0
	18.07.1997	Landsat 5	TM	WGS 84	UTM zone 36 N	30 × 30	180/032	GEOTIFF	0
	14.07.1998	Landsat 5	TM	WGS 84	UTM zone 36 N	30 × 30	179/032	GEOTIFF	0
	10.08.1999	Landsat 7	ETM	WGS 84	UTM zone 36 N	30 × 30	179/032	GEOTIFF	0
17 August 1999—Golcuk earthquake, Izmit, Turkey									
Post-earthquake	27.09.1999	Landsat 7	ETM	WGS 84	UTM zone 36 N	30 × 30	179/032	GEOTIFF	0
	25.06.2000	Landsat 7	ETM	WGS 84	UTM zone 36 N	30 × 30	179/032	GEOTIFF	0
	06.07.2004	Landsat 7	ETM	WGS 84	UTM zone 36 N	30 × 30	179/032	GEOTIFF	1
	02.08.2008	Landsat 7	ETM	WGS 84	UTM zone 36 N	30 × 30	179/032	GEOTIFF	2
	24.06.2011	Landsat 7	ETM	WGS 84	UTM zone 36 N	30 × 30	179/032	GEOTIFF	0
	21.07.2015	Landsat 7	ETM	WGS 84	UTM zone 36 N	30 × 30	179/032	GEOTIFF	2
	24.06.2017	Landsat 7	ETM	WGS 84	UTM zone 36 N	30 × 30	179/032	GEOTIFF	8

study, events which were thought to have affected the coastal change (earthquakes, etc.) were taken into consideration. To determine changes before and after the 17 August 1999 earthquake and the effects of this earthquake on the coast, the images dated 1999 August 10 and 1999 September 27 and having appropriate parameters were also added to the dataset.

Processing of satellite images and the automatic extraction of shorelines

Firstly, the pre-processing steps, which include atmospheric correction and radiometric correction stages, were applied to satellite images. Afterward, for the accurate extraction of shorelines from Landsat satellite images of a total of 17 periods between 1975 and 2017, noises in the images were reduced by applying the minimum noise fraction (MNF) transformation, which is used effectively in the literature (Ayoobi and Tangestani 2017; Lixin et al. 2015; Ceylan 2012). Since the spatial resolution of multispectral bands in Landsat images is 30 m, mixed pixels are formed in the transition zones between water and land. Traditional classification methods cause the misclassification of mixed pixels by assigning each pixel to a single class, and this causes the

reduction of the accuracy of classification (Ceylan 2012). Therefore, the matched filter (Fereydooni and Mojeddifar 2017; Ceylan 2012) subpixel analysis was applied to extract the shoreline from Landsat images. There are settlements, roads, and water areas within the study area. These classes, which are of different types, have different reflection and texture values that can be used in classification algorithms (Kahya 2005). Texture analysis (Ferreira et al. 2019) was applied to the abundant images created in this context, and the shoreline was obtained as raster data.

Automatic shoreline extraction is extremely important because, if the study area is large and very indented, it may take a long time to extract the shoreline manually. For example, our study area is very large and indented, and it has a shoreline of approximately 130 km. At the same time, manual extraction of the shoreline of 17 periods will result in considerable time loss. To obtain shorelines as vector data and extract them automatically, the method developed by Cırtıcı (2020) was used. Steps involving all of these processes (minimum noise fraction, matched filter, and texture analysis) were followed, and the shorelines were created as raster data. Finally, vector shorelines were generated automatically by the method developed (Cırtıcı 2020).

Shoreline change analysis

It is possible to divide the Gulf of Izmit, which has a tectonic formation, geographically into three sections: eastern, middle, and western (Ceylan 2012). In coastal change analysis studies, the investigation of the study area by dividing it into sections provides the opportunity for a better interpretation of analysis results. At the same time, while the coasts to the east and west of the Gulf of Izmit have a rather indented structure, the central section has a flatter structure. For this reason, the study area was examined by dividing it into three regions (Fig. 1). Zone 1 is the region in the eastern part, which was very close to the epicenter of the 17 August 1999 earthquake and where the amount of erosion after the earthquake reached the maximum value. While zone 2 represents the middle section, zone 3 represents the western section.

Episodic shoreline retreat should definitely be taken into account in coastal change analysis. In this study, when the satellite image periods used for coastal change analysis were examined (Table 1), an earthquake of 7.4 magnitude was observed to occur in the study area on 17 August 1999. This earthquake caused the sea to enter into the inland in many locations, especially in Gölcük district. Therefore, the coastal change analysis in the study area was carried out in two different periods, as pre-earthquake (1975/06/17–1999/08/10) and post-earthquake (1999/09/27–2017/06/24). However, the 42-year change that occurred between 1975 and 2017 was also analyzed. On the other hand, changes that occurred between 1997 July 18 and 1999 August 10 and between 1997 July 18 and 1999 September 27 due to the episodic shoreline retreat caused by the earthquake of 1999 August 17 were also analyzed.

In this study, coastal changes were analyzed in a 95% confidence interval using the EPR, LRR, and WLR statistical methods in the ArcGIS 10.5-DSAS 5.0 software. In the analysis, a baseline was created parallel to the shorelines and at a distance of approximately 500 m in the sea direction. On the baseline, which was approximately 130 km long, a total of 1164 transects were produced at 100-m intervals. Of the 1164 transects produced, 320 were located in zone 1, 397 were located in zone 2, and 447 were located in zone 3.

End point rate method

In the end point rate (EPR method, calculations are performed by dividing the total distance of shoreline change

by the elapsed time difference. The EPR method performs calculations by using the shoreline belonging to two different dates. If there are more than two shorelines, the EPR method is used to make calculations for different combinations. EPR is widely used because it is an easily applicable method (Dolan et al. 1991; Crowell et al. 1997).

$$EPR = \frac{(d_1 - d_0)}{(t_1 - t_0)} m/year \quad EPR = \frac{(d_{2017} - d_{1975})}{(t_{2017} - t_{1975})} m/year$$

Linear regression rate method

In the linear regression rate (LRR) method, it is aimed to fit the most suitable regression line for each transect intersecting all shorelines. The least squares method is used for the line calculation. In this method, all shorelines used in the study are taken into account, and distance variables are used together with time for coastal change analysis. The time specified here is the year information of the shoreline. For each transect, the variable specified as the distance is the distance from the beginning of the baseline to the point at which the transect intersects shorelines. The slope of the formed line provides the coastal change rate. Therefore, it is a more sensitive method than other coastal change rate calculation methods. Some advantages of the method are as follows:

- The method is based on a previously accepted statistical method.
- It is a method easy to use and understand and consists of a simple calculation.
- All shorelines used in the study are taken into account.
- The accuracy of the calculated coastal change rate depends on the accuracy of obtaining shorelines, temporal coastal changes, and the number of data used in the calculation (Dolan et al. 1991; Genz et al. 2007).

Weighted linear regression rate method

In the weighted linear regression (WLR) method, importance is attached to the fact that there is more data or weight to determine the optimal regression line. All shorelines used in the study are taken into account, and the distance variables are used together

with time for coastal change analysis. The time specified here is the year information of the shoreline. For each transect, the variable specified as the distance is the distance from the beginning of the baseline to the point at which the transect intersects shorelines. However, shoreline measurement points with small spatial uncertainty values have more impact on the regression calculation due to the weighting component in the algorithm. The slope of the regression line gives the coastal change rate. The WLR method is also a sensitive method, similar to the LRR method (Genz et al. 2007).

Results and discussion

The LRR and WLR methods used in this study are similar methods and require at least three periods of the shoreline. In the EPR method, coastal change analysis can be performed with two periods of the shoreline. The results of the analysis were interpreted according to the LRR method preferred by various researchers (Crowell et al. 1997; Maiti and Bhattacharya 2009; Güneröglu 2015) because the LRR method minimizes the effect of random error and short-term changes.

The analyses were carried out by considering four different scenarios.

Scenario 1

Firstly, the 42-year change, which occurred between 1975 June 14 and 2017 June 24, was analyzed with all three methods by using satellite images of 15 periods (the satellite images dated 1999/08/10 and 1999/09/27 were not taken into account due to the possibility of misleading results because of the earthquake that occurred in 1999). According to the LRR method, maximum erosion was obtained to be -13.91 m/year in zone 1, -1.83 m/year in zone 2, and -11.63 m/year in zone 3, and maximum accretion was obtained to be 12.12 m/year in zone 1, 12.01 m/year in zone 2, and 12.87 m/year in zone 3 at the end of 42 years in the study area (Table 2).

Scenario 2

In this scenario, pre-earthquake (1975/06/17–1999/08/10) and post-earthquake (1999/09/27–2017/06/24) shoreline changes due to the episodic shoreline retreat

were calculated using all three methods (Figs. 3, 4, and 5). As a result of this analysis, maximum erosion, which occurred within the 24 years before the earthquake (1975–1999) and was calculated using the LRR method, was -5.78 m/year in zone 1, -1.86 m/year in zone 2, and -3.32 m/year in zone 3, and maximum accretion calculated using the LRR method was 28.78 m/year in zone 1, 5.06 m/year in zone 2, and 8.81 m/year in zone 3. Maximum erosion, which occurred within the 18 years (1999–2017) after the earthquake and was calculated using the LRR method, was -27.92 m/year in zone 1, -5.65 m/year in zone 2, and -6.68 m/year in zone 3, and maximum accretion was 17.36 m/year in zone 1, 37.69 m/year in zone 2, and 30.24 m/year in zone 3 (Tables 3 and 4).

Scenario 3

To examine the impact of the pre-earthquake and post-earthquake process on the shoreline, within this scenario, two different strategies were followed, and various analyses were conducted. In the first strategy, the Landsat satellite image (1999/08/10) just before the earthquake was accepted as a reference image and analyzed using all three methods by starting from 1975 and excluding the image with the oldest date at each time (Table 3, Figs. 3 and 4). In the post-earthquake analysis, the Landsat satellite image (2017/06/24) was accepted as a reference image, and the same strategy was applied by excluding the image with the oldest date (starting from 1999/09/27) at each time (Table 4 and Fig. 5). The comparison values were interpreted according to the LRR method due to the strategy followed during the coastal change analysis before and after the earthquake (excluding the image with the oldest date at each time). Thus, when exactly the coast underwent an extreme change can be revealed more clearly.

Figure 6 explains the map showing in which period and where the maximum amount of erosion occurred in the study area before and after the earthquake. Since maximum values were obtained in the same transects in all three methods, maps were created using one method (Fig. 6).

Scenario 4

In addition to these analyses, in contrast to the previous strategy for the analysis of coastal change before and

Table 2 Erosion/accretion values (the max. and average) in 42 years (between 1975/06/17 and 2017/06/24)

THE COMPARISON MAX. EROSION / ACCRETION BETWEEN 1975/06/17 AND 2017/06/24						
Date of Image	ZONE 1		ZONE 2		ZONE 3	
	EPR		EPR		EPR	
	EROSION	ACCRETION	EROSION	ACCRETION	EROSION	ACCRETION
	Max. Value (m/year)	Max. Value (m/year)	Max. Value (m/year)	Max. Value (m/year)	Max. Value (m/year)	Max. Value (m/year)
1975/06/17-2017/06/24	-9.33	14.65	-2.84	14.78	-9.82	12.18
	LRR		LRR		LRR	
	EROSION	ACCRETION	EROSION	ACCRETION	EROSION	ACCRETION
	Max. Value (m/year)	Max. Value (m/year)	Max. Value (m/year)	Max. Value (m/year)	Max. Value (m/year)	Max. Value (m/year)
1975/06/17-2017/06/24	-13.91	12.12	-1.83	12.01	-11.63	12.87
	WLR		WLR		WLR	
	EROSION	ACCRETION	EROSION	ACCRETION	EROSION	ACCRETION
	Max. Value (m/year)	Max. Value (m/year)	Max. Value (m/year)	Max. Value (m/year)	Max. Value (m/year)	Max. Value (m/year)
1975/06/17-2017/06/24	-18.92	26.51	-2.93	6.47	-6.1	12.78
THE COMPARISON AVERAGE EROSION / ACCRETION BETWEEN 1975/06/17 AND 2017/06/24						
Date of Image	ZONE 1		ZONE 2		ZONE 3	
	EPR		EPR		EPR	
	EROSION (m/year)	ACCRETION (m/year)	EROSION (m/year)	ACCRETION (m/year)	EROSION (m/year)	ACCRETION (m/year)
1975/06/17-2017/06/24	-1.43	1.92	-0.62	1.43	-0.89	3.08
	LRR		LRR		LRR	
	EROSION (m/year)	ACCRETION (m/year)	EROSION (m/year)	ACCRETION (m/year)	EROSION (m/year)	ACCRETION (m/year)
	Max. Value (m/year)	Max. Value (m/year)	Max. Value (m/year)	Max. Value (m/year)	Max. Value (m/year)	Max. Value (m/year)
1975/06/17-2017/06/24	-1.34	1.9	-0.46	1.39	-0.69	3.24
	WLR		WLR		WLR	
	EROSION (m/year)	ACCRETION (m/year)	EROSION (m/year)	ACCRETION (m/year)	EROSION (m/year)	ACCRETION (m/year)
	Max. Value (m/year)	Max. Value (m/year)	Max. Value (m/year)	Max. Value (m/year)	Max. Value (m/year)	Max. Value (m/year)
1975/06/17-2017/06/24	-1.44	2.76	-0.85	1.49	-1.15	2.06

after the earthquake, Landsat satellite images (1997/07/18 and 1975/06/17) were accepted as a reference image, and the analyses were made by considering the satellite images immediately before (1999/08/10) and immediately after the earthquake (1999/09/27). Within the scope of this scenario, the pre- and post-earthquake images were analyzed using all three methods to determine the impact on the shoreline after the earthquake occurred. Values related to this analysis are presented in Table 5.

In the pre-earthquake period in which the year 1975 was taken as a reference, the maximum erosion amounts calculated using the LRR method were -5.46 m/year in zone 1, -1.65 m/year in zone 2, and -3.26 m/year in zone 3, and the maximum accretion amounts were 29.83 m/year in zone 1, 5.62 m/year in zone 2, and 8.63 m/year in zone 3. In the pre-earthquake period in which the year 1997 was taken as a reference, the maximum erosion amounts were calculated to be -59.54 m/year in zone 1, -38.95 m/year in zone 2, and -50.42 m/year in zone 3, while the maximum accretion amounts were obtained to be 105.33 m/year in zone 1, 30.25 m/year in zone 2, and 114.46 m/year in zone 3 (Table 5).

In the post-earthquake period in which the year 1975 was taken as a reference, while the maximum erosion

amounts were calculated using the LRR method as -4 m/year in zone 1, -1.93 m/year in zone 2, and -3.62 m/year in zone 3, the maximum accretion amounts were obtained to be 23.22 m/year in zone 1, 5.50 m/year in zone 2, and 9.75 m/year in zone 3. In the post-earthquake period in which the year 1997 was taken as a reference, while the maximum erosion amounts were calculated to be -151.51 m/year in zone 1, -28.18 m/year in zone 2, and -64.87 m/year in zone 3, the maximum accretion amounts were 57.06 m/year in zone 1, 25.12 m/year in zone 2, and 111.4 m/year in zone 3 (Table 5).

The epicenter of the earthquake, which occurred on 17 August 1999 with a magnitude of $M_w = 7.4$, is the Gölcük district of Kocaeli province. Since it was the epicenter of the earthquake, the most significant loss of life and property occurred in Gölcük. Particularly in Kavaklı Neighborhood, a large piece of land submerged together with the apartment building, road, swimming pool, sports facility, and amusement park on it. The amusement park, which submerged in this area, is one of the symbols of the disaster (Fig. 7). After the earthquake, this area was turned into a green area, and construction was not allowed (Doğan News Agency 2019). At the same time, the Mayor of Gölcük stated in an interview to a

The comparison chart of EPR-LRR-WLR values

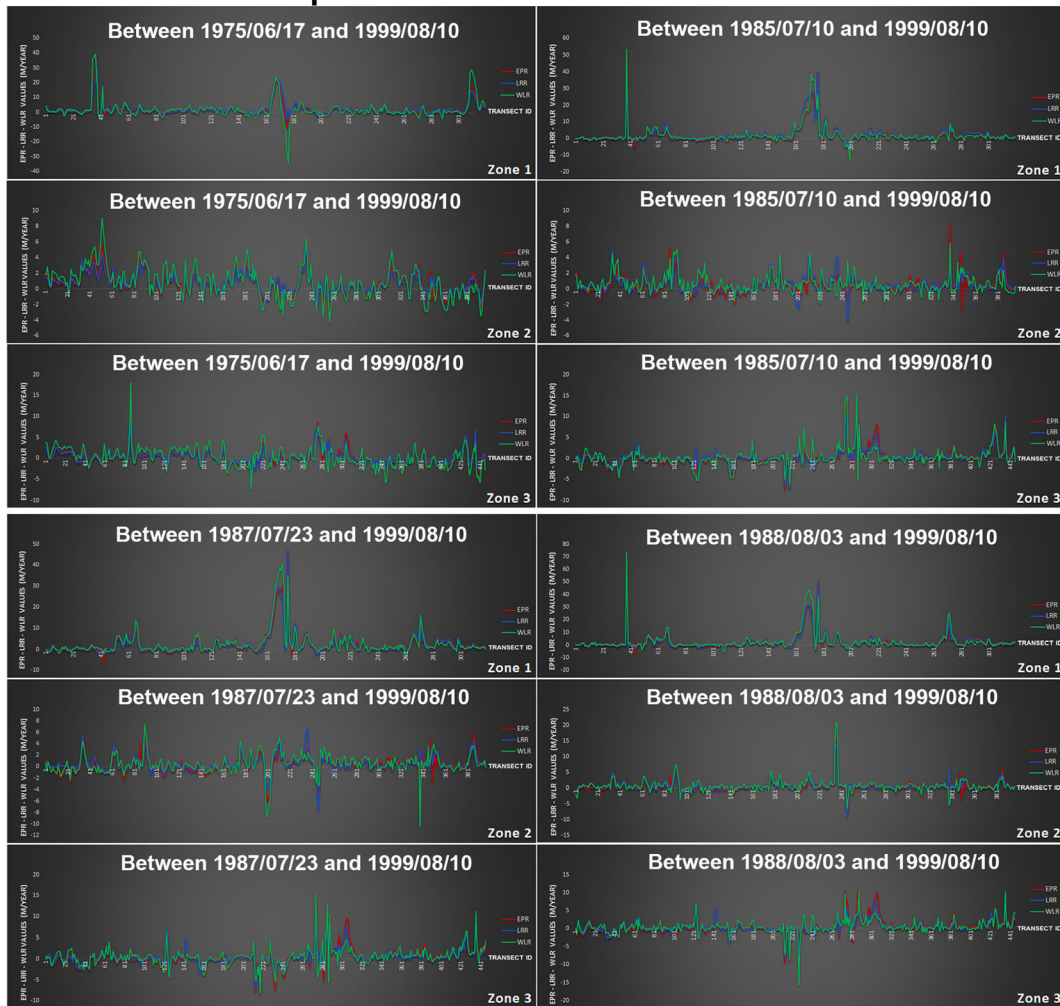


Fig. 3 Shoreline change values (meter/year) calculated using the EPR, LRR, and WLR methods in the pre-earthquake period (1975–1985–1987–1988 and 1999)

newspaper that he experienced the earthquake in his house on the coast of Kavaklı Neighborhood and found himself in the sea when he went out. He emphasized that the sea entered hundreds of meters inwards (Vatan Newspaper 2015). On the other hand, as a result of the earthquake, the land in the Kavaklı region of Gölcük district, which is an alluvial field, subsided around 1–1.5 m, and seawater entered inland for about 100 m. Together with the land used as a recreation area in terms of coastal use, the Olympic-sized swimming pool, football field, and other sports areas in this area also submerged (Uzun and

Garipagaoglu 2014). The shorelines obtained from Landsat satellite images dated 1999 August 10 and 1999 September 27 just before and after the earthquake were compared in this area, and it was measured that the sea entered inland for approximately 95 m (Fig. 7). As a result, this study confirms the previously mentioned coastal change studies in this area (Uzun and Garipagaoglu 2014; Doğan News Agency 2019; Vatan Newspaper 2015) and field observations after the earthquake.

The determination of the temporal change in the shoreline is essential for sustainable coastal

The comparison chart of EPR-LRR-WLR values

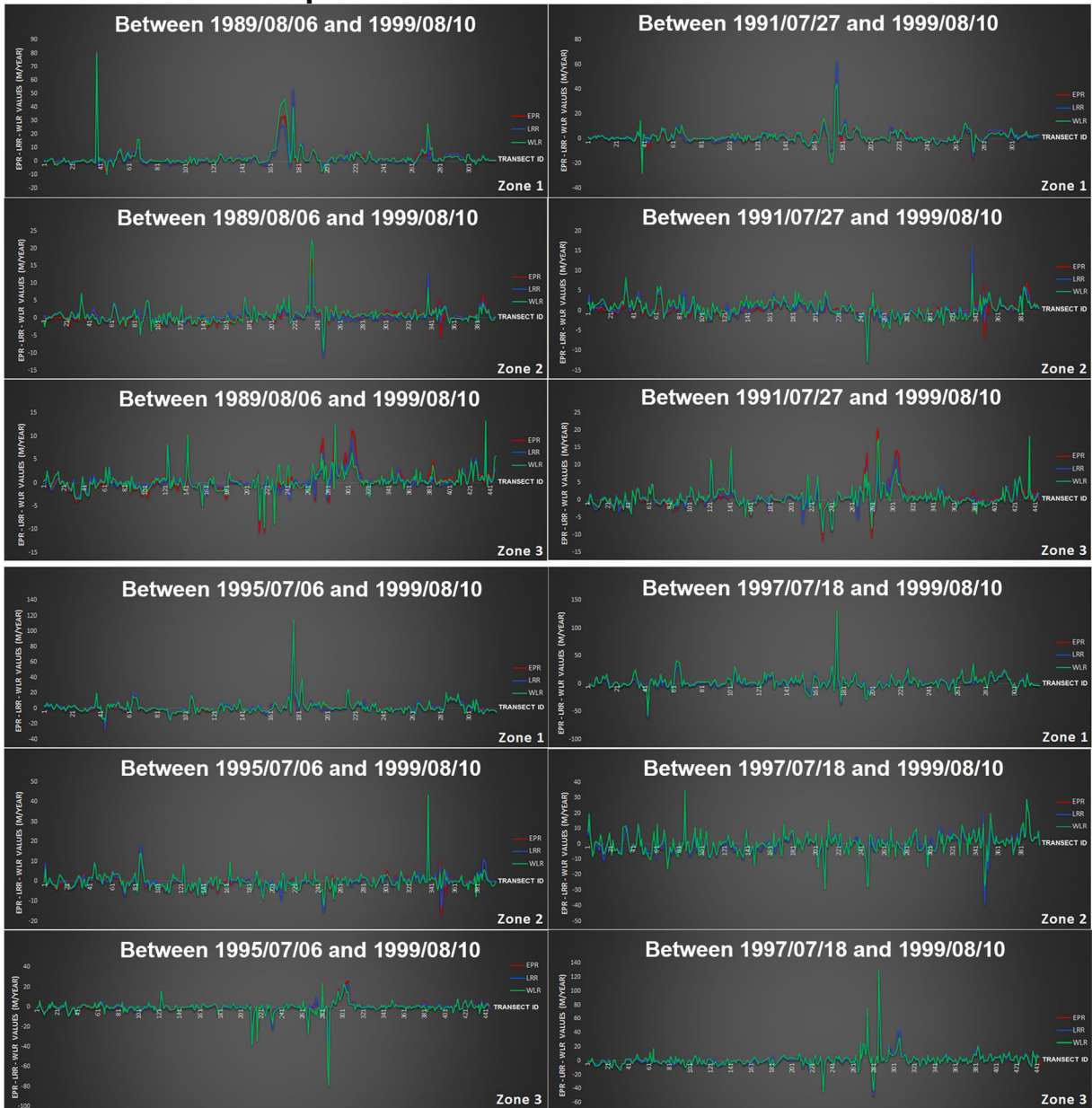


Fig. 4 Shoreline change values (meter/year) calculated using the EPR, LRR, and WLR methods in the pre-earthquake period (1989–1991–1995–1997 and 1999)

development and planning. To detect this change, satellite images, which provide a regular data source for the past, play an important role. Therefore, in this study, temporal changes in coastal areas were monitored by using Landsat satellite images between 1975 and 2017, and coastal changes in the Gulf of Izmit were attempted to be determined. Although shoreline

change rates are given as annual rates, they must be taken into consideration as “average” annual rates. A particular shoreline with a long-term retreat rate of 2 m/year would be expected to be 120 m landward in 60 years. A single storm/tsunami, however, could cause much of this movement (Gibeaut, 2001). The studies on coastal changes caused by earthquakes,

The comparison chart of EPR-LRR-WLR values

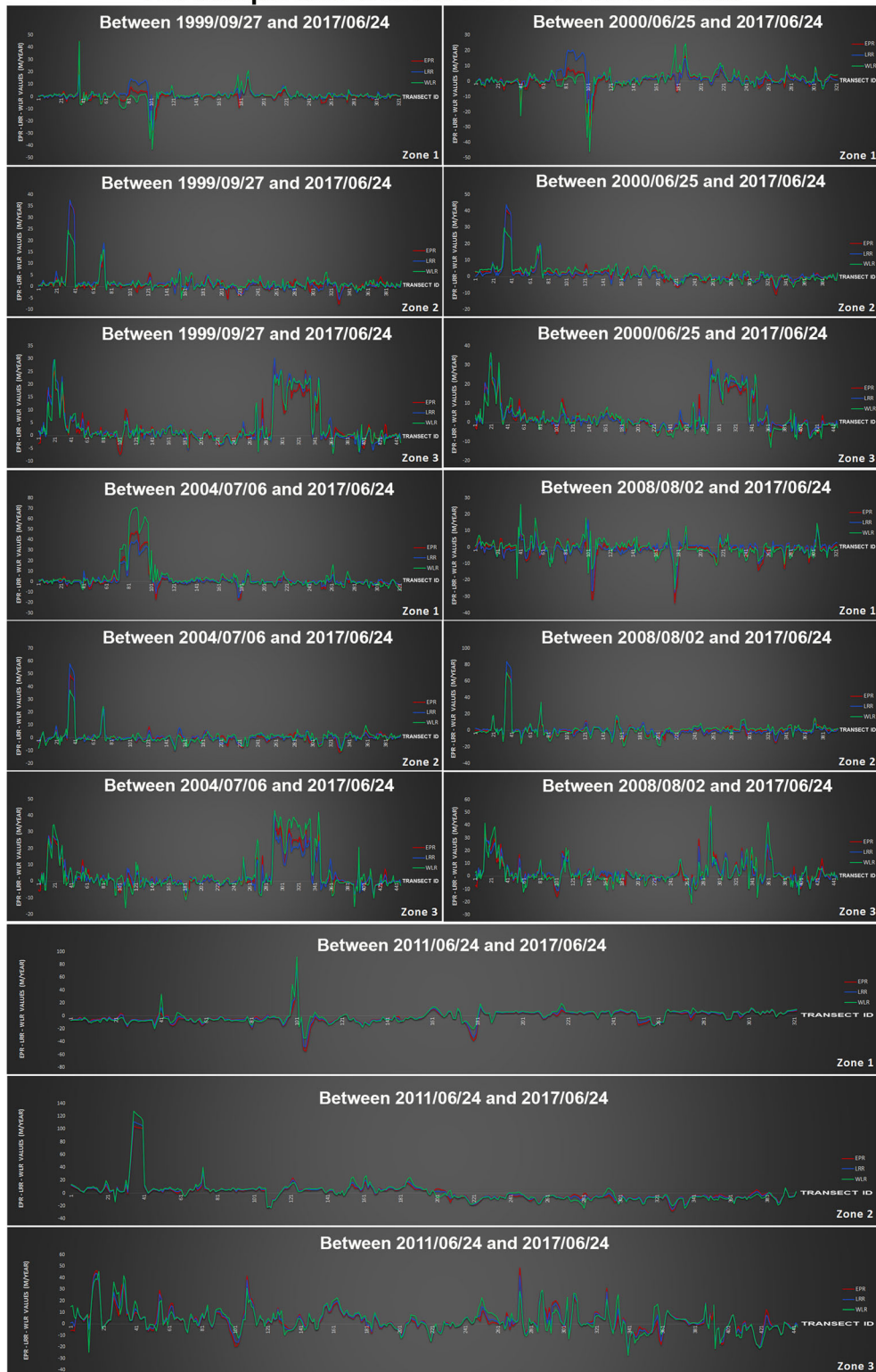


Fig. 5 Shoreline change values (meter/year) calculated using the EPR, LRR, and WLR methods in the post-earthquake period (1999–2000–2004–2008–2011 and 2017)

Table 3 Erosion/accretion values (the max. and average) before the earthquake (between 1975/06/17 and 1999/08/10)

THE COMPARISON MAX. EROSION / ACCRETION FOR PRE-EARTHQUAKE (1975/06/17-1999/08/10)						
Date of Image	ZONE 1		ZONE 2		ZONE 3	
	EPR		EPR		EPR	
	EROSION	ACCRETION	EROSION	ACCRETION	EROSION	ACCRETION
	Max. Value (m/year)	Max. Value (m/year)	Max. Value (m/year)	Max. Value (m/year)	Max. Value (m/year)	Max. Value (m/year)
1975/06/17-1999/08/10	-10.71	24.28	-2.6	5.77	-4.16	11.44
1985/07/10-1999/08/10	-9.73	41.58	-2.79	8.43	-7.58	14.63
1987/07/23-1999/08/10	-6.89	47.09	-6.12	5.87	-8.56	14.09
1988/08/03-1999/08/10	-6.71	56.07	-7.69	15.4	-12.2	10.58
1989/08/06-1999/08/10	-7.56	58.5	-9.84	16.95	-10.67	11.37
1991/07/27-1999/08/10	-18.86	59.29	-12.26	13.1	-11.58	20.72
1995/07/06-1999/08/10	-29.7	105.89	-16.84	32.6	-34.87	26.01
1997/07/18-1999/08/10	-59.4	106.43	-38.44	30.43	-50.06	115.1
	LRR		LRR		LRR	
	EROSION	ACCRETION	EROSION	ACCRETION	EROSION	ACCRETION
	Max. Value (m/year)	Max. Value (m/year)	Max. Value (m/year)	Max. Value (m/year)	Max. Value (m/year)	Max. Value (m/year)
1975/06/17-1999/08/10	-5.78	28.78	-1.86	5.06	-3.32	8.81
1985/07/10-1999/08/10	-5.9	40.13	-4.07	5.07	-7.29	10.52
1987/07/23-1999/08/10	-2.71	46.53	-7.94	6.65	-7.63	11.15
1988/08/03-1999/08/10	-4.17	66.72	-9.37	14.28	-8.02	10.62
1989/08/06-1999/08/10	-4.81	64.85	-11.14	12.54	-8.07	11.61
1991/07/27-1999/08/10	-20.87	63.43	-13.11	15.71	-9.4	11.98
1995/07/06-1999/08/10	-28	112.56	-15.49	32.92	-38.09	22.48
1997/07/18-1999/08/10	-59.54	105.33	-38.95	30.25	-50.42	114.46
	WLR		WLR		WLR	
	EROSION	ACCRETION	EROSION	ACCRETION	EROSION	ACCRETION
	Max. Value (m/year)	Max. Value (m/year)	Max. Value (m/year)	Max. Value (m/year)	Max. Value (m/year)	Max. Value (m/year)
1975/06/17-1999/08/10	-34.39	39.48	-4.24	9.07	-7.36	17.99
1985/07/10-1999/08/10	-13.09	53.31	-1.79	5.88	-6.44	15.29
1987/07/23-1999/08/10	-9.38	40.58	-10.33	7.41	-8.12	15.3
1988/08/03-1999/08/10	-5.13	73.89	-6.45	20.83	-15.76	10.19
1989/08/06-1999/08/10	-10.03	80.57	-9.39	22.37	-9.6	13.21
1991/07/27-1999/08/10	-27.95	43.97	-12.85	9.19	-9.22	18.29
1995/07/06-1999/08/10	-16.39	114.89	-12.26	43.17	-78.94	23.2
1997/07/18-1999/08/10	-56.37	130.49	-29.36	34.48	-44.75	129.05
THE COMPARISON AVERAGE EROSION / ACCRETION FOR PRE-EARTHQUAKE (1975/06/17-1999/08/10)						
Date of Image	ZONE 1		ZONE 2		ZONE 3	
	EPR		EPR		EPR	
	EROSION (m/year)	ACCRETION (m/year)	EROSION (m/year)	ACCRETION (m/year)	EROSION (m/year)	ACCRETION (m/year)
1975/06/17-1999/08/10	-1.12	2.85	-0.7	1.34	-0.96	1.38
1985/07/10-1999/08/10	-1.05	2.88	-0.46	0.93	-0.98	1.26
1987/07/23-1999/08/10	-0.78	3.54	-0.88	1.18	-1.15	1.54
1988/08/03-1999/08/10	-0.89	3.84	-0.67	1.03	-0.97	1.36
1989/08/06-1999/08/10	-1.29	4.09	-0.87	1.45	-1.22	1.64
1991/07/27-1999/08/10	-1.95	3.49	-1.14	1.28	-1.4	2
1995/07/06-1999/08/10	-2.69	5.51	-2.14	2.06	-2.44	2.85
1997/07/18-1999/08/10	-5.23	7.63	-4.28	4.27	-4.02	6.11
	LRR		LRR		LRR	
	EROSION (m/year)	ACCRETION (m/year)	EROSION (m/year)	ACCRETION (m/year)	EROSION (m/year)	ACCRETION (m/year)
	Max. Value (m/year)	Max. Value (m/year)	Max. Value (m/year)	Max. Value (m/year)	Max. Value (m/year)	Max. Value (m/year)
1975/06/17-1999/08/10	-0.82	2.74	-0.6	1.16	-0.86	1.26
1985/07/10-1999/08/10	-0.65	3.21	-0.43	0.92	-0.78	1.13
1987/07/23-1999/08/10	-0.71	3.42	-0.61	1.05	-0.86	1.29
1988/08/03-1999/08/10	-0.81	3.87	-0.53	1.05	-0.76	1.28
1989/08/06-1999/08/10	-0.94	3.98	-0.66	1.16	-0.93	1.45
1991/07/27-1999/08/10	-1.79	3.71	-0.99	1.41	-1.38	1.75
1995/07/06-1999/08/10	-2.75	5.73	-2.15	1.97	-2.62	2.6
1997/07/18-1999/08/10	-4.99	7.57	-4.28	4.25	-3.99	6.14
	WLR		WLR		WLR	
	EROSION (m/year)	ACCRETION (m/year)	EROSION (m/year)	ACCRETION (m/year)	EROSION (m/year)	ACCRETION (m/year)
	Max. Value (m/year)	Max. Value (m/year)	Max. Value (m/year)	Max. Value (m/year)	Max. Value (m/year)	Max. Value (m/year)
1975/06/17-1999/08/10	-2.15	3.71	-1.14	1.84	-1.51	1.94
1985/07/10-1999/08/10	-0.89	2.99	-0.42	1.01	-1.02	1.4
1987/07/23-1999/08/10	-0.73	3.58	-0.91	1.29	-1.27	1.45
1988/08/03-1999/08/10	-0.79	4.11	-0.79	1.23	-0.92	1.23
1989/08/06-1999/08/10	-1.28	4.51	-0.9	1.66	-1.12	1.48
1991/07/27-1999/08/10	-2.26	3.52	-1.43	1.72	-1.28	2.09
1995/07/06-1999/08/10	-3.21	6.1	-2.13	2.58	-3.43	2.7
1997/07/18-1999/08/10	-6.5	8.98	-4.66	4.87	-4.33	6.17

Table 4 Erosion/accretion values (the max. and average) after the earthquake (between 1999/09/27 and 2017/06/24)

THE COMPARISON MAX. EROSION / ACCRETION FOR POST-EARTHQUAKE (1999/09/27-2017/06/24)						
Date of Image	ZONE 1		ZONE 2		ZONE 3	
	EPR		EPR		EPR	
	EROSION	ACCRETION	EROSION	ACCRETION	EROSION	ACCRETION
	Max. Value (m/year)	Max. Value (m/year)	Max. Value (m/year)	Max. Value (m/year)	Max. Value (m/year)	Max. Value (m/year)
1999/09/27-2017/06/24	-28.95	32.9	-7.72	36.73	-7.41	28.47
2000/06/25-2017/06/24	-30.57	16.41	-10.86	40.88	-7.65	29.4
2004/07/06-2017/06/24	-17.55	48.36	-10.98	49.53	-9.3	40.18
2008/08/02-2017/06/24	-33.97	11.94	-14.73	70.03	-15.91	47.01
2011/06/24-2017/06/24	-54.57	71.67	-28.3	104.27	-21.44	48.49
Date of Image	LRR		LRR		LRR	
	EROSION	ACCRETION	EROSION	ACCRETION	EROSION	ACCRETION
	Max. Value (m/year)	Max. Value (m/year)	Max. Value (m/year)	Max. Value (m/year)	Max. Value (m/year)	Max. Value (m/year)
	1999/09/27-2017/06/24	-27.92	17.36	-5.65	37.69	-6.68
2000/06/25-2017/06/24	-22.43	20.42	-7.51	43.91	-8.03	32.69
2004/07/06-2017/06/24	-15.59	39.84	-9.87	58.05	-8.15	41.43
2008/08/02-2017/06/24	-27.67	19.38	-13.21	84.09	-14.68	43.38
2011/06/24-2017/06/24	-47.93	78.21	-25.63	111.92	-23.34	43.7
Date of Image	WLR		WLR		WLR	
	EROSION	ACCRETION	EROSION	ACCRETION	EROSION	ACCRETION
	Max. Value (m/year)	Max. Value (m/year)	Max. Value (m/year)	Max. Value (m/year)	Max. Value (m/year)	Max. Value (m/year)
	1999/09/27-2017/06/24	-42.91	44.89	-5.2	24.56	-6.91
2000/06/25-2017/06/24	-45.73	24.41	-6.53	29.86	-13.11	36.37
2004/07/06-2017/06/24	-8.13	70.85	-10.21	37.22	-16.02	42.96
2008/08/02-2017/06/24	-25.8	26.02	-18.9	70.89	-20.7	54.83
2011/06/24-2017/06/24	-34.21	91.72	-23.92	127.73	-27.28	45.22
THE COMPARISON AVERAGE EROSION / ACCRETION FOR POST-EARTHQUAKE (1999/09/27-2017/06/24)						
Date of Image	ZONE 1		ZONE 2		ZONE 3	
	EPR		EPR		EPR	
	EROSION (m/year)	ACCRETION (m/year)	EROSION (m/year)	ACCRETION (m/year)	EROSION (m/year)	ACCRETION (m/year)
1999/09/27-2017/06/24	-2.74	1.77	-1.14	2.26	-1.41	6.02
2000/06/25-2017/06/24	-3	2.68	-1.82	3.9	-2.28	7.53
2004/07/06-2017/06/24	-2.22	6.3	-2.01	3.1	-1.87	8.97
2008/08/02-2017/06/24	-3.7	2.13	-3.37	4.41	-3.02	7
2011/06/24-2017/06/24	-7.63	5.44	-6.9	9.48	-5.31	7.81
Date of Image	LRR		LRR		LRR	
	EROSION (m/year)	ACCRETION (m/year)	EROSION (m/year)	ACCRETION (m/year)	EROSION (m/year)	ACCRETION (m/year)
	1999/09/27-2017/06/24	-1.72	2.91	-0.98	2.59	-1.39
2000/06/25-2017/06/24	-1.82	3.62	-1.52	3.14	-1.77	7.72
2004/07/06-2017/06/24	-1.63	5.89	-1.95	3.48	-1.87	7.68
2008/08/02-2017/06/24	-3.51	2.39	-2.83	5.99	-2.77	6.5
2011/06/24-2017/06/24	-7.37	6.13	-7.22	10.06	-5.37	7.77
Date of Image	WLR		WLR		WLR	
	EROSION (m/year)	ACCRETION (m/year)	EROSION (m/year)	ACCRETION (m/year)	EROSION (m/year)	ACCRETION (m/year)
	1999/09/27-2017/06/24	-3.51	2.36	-0.76	2.2	-1.42
2000/06/25-2017/06/24	-3.34	3.73	-2	4.28	-3.05	7.75
2004/07/06-2017/06/24	-2.19	9.47	-2.3	3.39	-2.38	11.38
2008/08/02-2017/06/24	-3.32	3.5	-4.15	5.36	-3.3	7.73
2011/06/24-2017/06/24	-7.23	7.64	-8.41	11.39	-5.77	8.68

tsunamis, and global climate change can provide useful information for understanding natural disasters. This issue can be explored in detail, regardless of the presence of a relationship between these events. If there is a relationship, it can be clarified after the methods used in this study are integrated with tectonic and meteorological data in a GIS environment.

Conclusions

One of the factors causing shoreline changes is the earthquake. The earthquake of 7.4 magnitude that occurred on 17 August 1999 had a great impact on the coasts of the Gulf of Izmit. Since this area is located on the NAFZ, which is one of the most active fault zones in the world, these effects are also likely

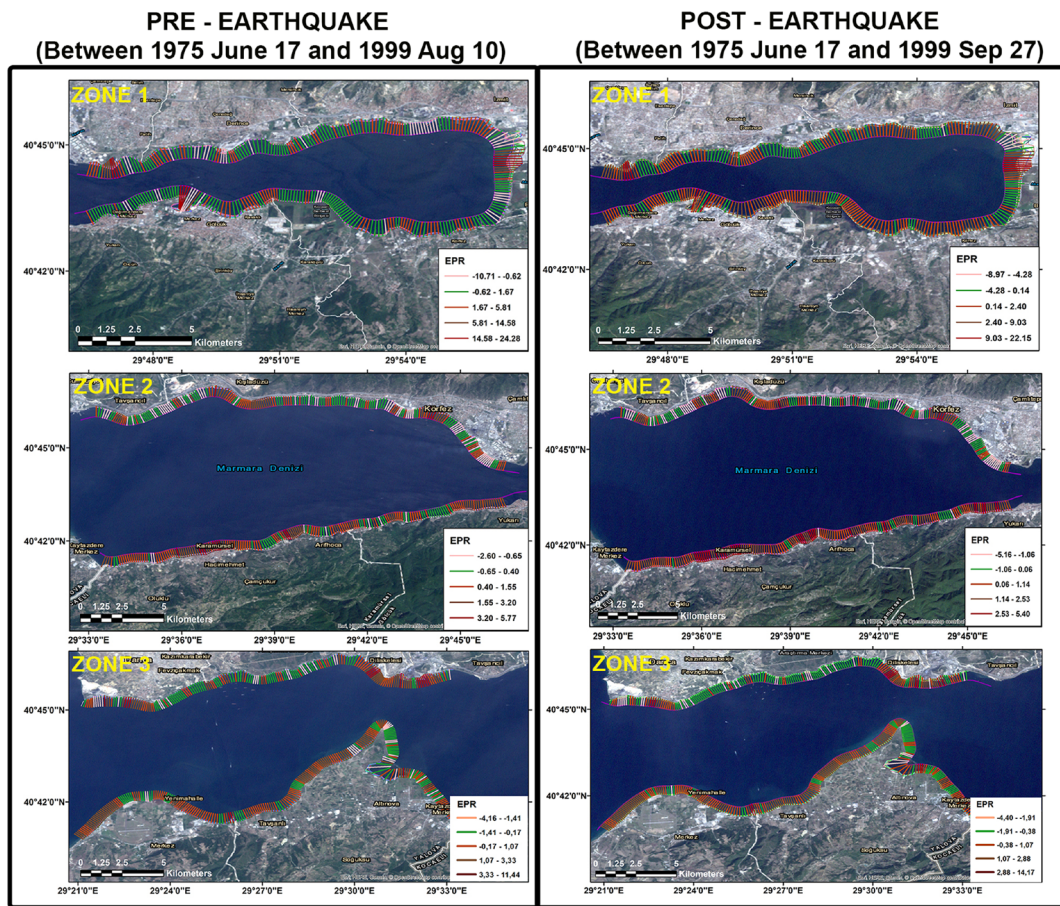


Fig. 6 The maximum amount of erosion/accretion that occurred before and after the earthquake

to occur in the future. Another situation that causes the shoreline on the coasts of the Gulf of Izmit to change is tsunamis that have occurred or may occur. Although there is a low probability of tsunami formation in the Marmara Sea, which is an inland sea, reasons, such as the effect of reverse faults, the magnitude and depth of earthquakes, and subsidence that may occur under the sea, indicate the existence of such a possibility (Altınok and Alpar 2010). For this reason, the management and use of coasts located in areas, which are at risk for natural disasters, are extremely important in terms of the loss of life and property.

Coastal areas are always subject to change since they have a lot of resources, they are in the area of interaction of the land and sea environment, and they

are areas where many factors are effective. Coastal areas should be considered as a whole since they cover both land and water. As a result of the 17 August 1999 earthquake that occurred in the south of the Gulf of Izmit and affected the entire coasts of the gulf, alluvial fields, the areas through which the fault lines passed, and fill areas subsided, and seawater moved towards the inland. As a result, coastal changes occurred. In this research, the 42-year coastal change between 1975 and 2017 was analyzed using the EPR, LRR, and WLR statistical methods, and studies were also carried out to determine the effects of the earthquake that occurred on 17 August 1999 using GIS and remote sensing methods.

Accordingly, the shoreline, which has changed from past to present, is constantly under the influence of

Table 5 Maximum and average erosion/accretion values that occurred before and after the earthquake

PRE / POST EARTHQUAKE : MAX. EROSION / ACCRETION BETWEEN 1975/06/17 AND 1999/09/27						
Date of Image	ZONE 1		ZONE 2		ZONE 3	
	EPR		EPR		EPR	
	EROSION	ACCRETION	EROSION	ACCRETION	EROSION	ACCRETION
	Max. Value (m/year)	Max. Value (m/year)	Max. Value (m/year)	Max. Value (m/year)	Max. Value (m/year)	Max. Value (m/year)
1975/06/17-1999/08/10	-10.71	24.28	-2.6	5.77	-4.16	11.44
1975/06/17-1999/09/27	-8.97	22.15	-5.16	5.4	-4.4	14.17
	LRR		LRR		LRR	
	EROSION	ACCRETION	EROSION	ACCRETION	EROSION	ACCRETION
	Max. Value (m/year)	Max. Value (m/year)	Max. Value (m/year)	Max. Value (m/year)	Max. Value (m/year)	Max. Value (m/year)
1975/06/17-1999/08/10	-5.46	29.83	-1.65	5.62	-3.26	8.63
1975/06/17-1999/09/27	-4	23.22	-1.93	5.5	-3.62	9.75
	WLR		WLR		WLR	
	EROSION	ACCRETION	EROSION	ACCRETION	EROSION	ACCRETION
	Max. Value (m/year)	Max. Value (m/year)	Max. Value (m/year)	Max. Value (m/year)	Max. Value (m/year)	Max. Value (m/year)
1975/06/17-1999/08/10	-37.69	41.29	-4.49	9.56	-7.69	18.71
1975/06/17-1999/09/27	-38.67	37.58	-4.69	9.3	-7.3	19.01
PRE / POST EARTHQUAKE : AVERAGE EROSION / ACCRETION BETWEEN 1975/06/17 AND 1999/09/27						
Date of Image	ZONE 1		ZONE 2		ZONE 3	
	EPR		EPR		EPR	
	EROSION (m/year)	ACCRETION (m/year)	EROSION (m/year)	ACCRETION (m/year)	EROSION (m/year)	ACCRETION (m/year)
1975/06/17-1999/08/10	-1.12	2.85	-0.7	1.34	-0.96	1.38
1975/06/17-1999/09/27	-1.42	2.59	-0.94	1.44	-1.2	1.45
	LRR		LRR		LRR	
	EROSION (m/year)	ACCRETION (m/year)	EROSION (m/year)	ACCRETION (m/year)	EROSION (m/year)	ACCRETION (m/year)
1975/06/17-1999/08/10	-0.82	2.74	-0.6	1.16	-0.86	1.26
1975/06/17-1999/09/27	-0.77	2.53	-0.58	1.15	-0.82	1.22
	WLR		WLR		WLR	
	EROSION (m/year)	ACCRETION (m/year)	EROSION (m/year)	ACCRETION (m/year)	EROSION (m/year)	ACCRETION (m/year)
1975/06/17-1999/08/10	-2.15	3.71	-1.14	1.84	-1.51	1.94
1975/06/17-1999/09/27	-2.18	3.57	-1.19	1.88	-1.53	1.99
PRE / POST EARTHQUAKE : MAX. EROSION / ACCRETION BETWEEN 1997/07/18 AND 1999/09/27						
Date of Image	ZONE 1		ZONE 2		ZONE 3	
	EPR		EPR		EPR	
	EROSION	ACCRETION	EROSION	ACCRETION	EROSION	ACCRETION
	Max. Value (m/year)	Max. Value (m/year)	Max. Value (m/year)	Max. Value (m/year)	Max. Value (m/year)	Max. Value (m/year)
1997/07/18-1999/08/10	-59.4	106.43	-38.44	30.43	-50.06	115.1
1997/07/18-1999/09/27	-264.94	82.92	-49.37	24.47	-70.65	98.12
	LRR		LRR		LRR	
	EROSION	ACCRETION	EROSION	ACCRETION	EROSION	ACCRETION
	Max. Value (m/year)	Max. Value (m/year)	Max. Value (m/year)	Max. Value (m/year)	Max. Value (m/year)	Max. Value (m/year)
1997/07/18-1999/08/10	-59.54	105.33	-38.95	30.25	-50.42	114.46
1997/07/18-1999/09/27	-151.51	57.06	-28.18	25.12	-64.87	111.4
	WLR		WLR		WLR	
	EROSION	ACCRETION	EROSION	ACCRETION	EROSION	ACCRETION
	Max. Value (m/year)	Max. Value (m/year)	Max. Value (m/year)	Max. Value (m/year)	Max. Value (m/year)	Max. Value (m/year)
1997/07/18-1999/08/10	-56.37	130.49	-29.36	34.48	-44.75	129.05
1997/07/18-1999/09/27	-94.07	62.64	-29.32	25.45	-61.94	118.12
PRE / POST EARTHQUAKE : AVERAGE EROSION / ACCRETION BETWEEN 1997/07/18 AND 1999/09/27						
Date of Image	ZONE 1		ZONE 2		ZONE 3	
	EPR		EPR		EPR	
	EROSION (m/year)	ACCRETION (m/year)	EROSION (m/year)	ACCRETION (m/year)	EROSION (m/year)	ACCRETION (m/year)
1997/07/18 - 1999/08/10	-5.23	7.63	-4.28	4.27	-4.02	6.11
1997/07/18 - 1999/09/27	-10.25	10.96	-5.15	5.45	-6.26	5.41
	LRR		LRR		LRR	
	EROSION (m/year)	ACCRETION (m/year)	EROSION (m/year)	ACCRETION (m/year)	EROSION (m/year)	ACCRETION (m/year)
1997/07/18 - 1999/08/10	-4.99	7.57	-4.28	4.25	-3.99	6.14
1997/07/18 - 1999/09/27	-7.44	8.83	-3.74	4.1	-4.2	4.72
	WLR		WLR		WLR	
	EROSION (m/year)	ACCRETION (m/year)	EROSION (m/year)	ACCRETION (m/year)	EROSION (m/year)	ACCRETION (m/year)
1997/07/18 - 1999/08/10	-6.5	8.98	-4.66	4.87	-4.33	6.17
1997/07/18 - 1999/09/27	-6.46	7.87	-3.5	3.94	-3.59	5.29



Fig. 7 The location where the sea entered inland in the vicinity of Kavaklı neighborhood immediately after the earthquake, and the situation of the same area 15 years after the earthquake (adapted from Doğan News Agency 2019)

physical elements, such as geomorphological events, earthquakes, and tectonic movements. In recent years,

as a result of intensive human activities and intensive coastal use, the coasts have started to change also due to

human factors. These changes in shorelines have been the cause of many problems in coastal areas. If measures are not taken, the mentioned changes will continue to cause problems. Necessary measures can be taken in a short time and effectively using GIS and remote sensing techniques for sustainable coastal management.

Acknowledgments The authors would like to thank the United States Geological Survey (USGS) for the Landsat satellite images and DSAS 5.0 tool.

References

- Addo, K. A., Walkden, M., & Mills, J. P. (2008). Detection, measurement and prediction of shoreline recession in Accra, Ghana. *ISPRS Journal of Photogrammetry & Remote Sensing*, 63(5), 543–558. <https://doi.org/10.1016/j.isprsjprs.2008.04.001>.
- Alberti, A. P., Pires, A., & Freitas, L. ve Chaminé, H. (2013). Shoreline change mapping along the coast of Galicia, Spain. *Proceedings of the Institution of Civil Engineers – Maritime Engineering*, 166(3), 125–144. <https://doi.org/10.1680/maen.2012.23>.
- Altınok Y, Alpar B (2010) Marmara Tsunamileri, Olası Deniz içi Kaymaları ve Yerleşim Alanlarına Etkileri. *İstanbul'un Jeolojii Sempozyumu III Bildiriler Kitabı*.
- Arockiaraj, S., Kankara, R. S., Udhaba Dora, G., & Sathish, S. (2018). Estimation of seasonal morpho-sedimentary changes at headland bound and exposed beaches along South Maharashtra, west coast of India. *Environmental Earth Sciences*, 77(17), 604. <https://doi.org/10.1007/s12665-018-7790-y>.
- Ayoobi, I., & Tangestani, M. H. (2017). The effect of minimum noise fraction data input on success of artificial neural network in lithological mapping of a magmatic terrain with ASTER data; A case study from SE Iran. *Remote Sensing Applications Society and Environment*, 7, 21–26. <https://doi.org/10.1016/j.rsase.2017.06.001>.
- Beyazıt I (2014) Kızılırmak Deltasının Zamansal Kıyı Değişiminin Coğrafi Bilgi Sistemleri Ve Uzaktan Algılama Yöntemleri ile Belirlenmesi. Yıldız Teknik Üniversitesi Fen Bilimleri Enstitüsü, Yüksek Lisans Tezi.
- Ceylan, M., (2012). Uzaktan Algılama ve CBS ile Kıyı Çizgisi Değişiminin Belirlenmesi; İzmit Körfezi Örneği. Hava Harp Okulu Havacılık ve Uzay Teknolojileri Enstitüsü, Yüksek Lisans Tezi.
- Ciritçi, D., & Türk, T. (2019). Automatic detection of shoreline change by geographical information system (GIS) and remote sensing in the Göksu Delta, Turkey. *Journal of the Indian Society of Remote Sensing*, 47(2), 233–243. <https://doi.org/10.1007/s12524-019-00947-1>.
- Ciritçi D (2020) Automatic determination of the coastal change in the Gulf of İzmit by geographical information systems and remote sensing methods. Sivas Cumhuriyet University, Master Thesis (in Turkish).
- Crowell, M., Douglas, B. C., & Leatherman, S. P. (1997). On forecasting future U.S. shoreline positions—A test of algorithms. *Journal of Coastal Research*, 13(4), 1245–1255.
- Demirtaş, R. (2000). 17 Ağustos 1999 İzmit Körfezi Depremi Raporu. Bayındırlık ve İskan Bakanlığı Afet İşleri Genel Müdürlüğü Deprem Araştırma Dairesi Başkanlığı.
- Doğan News Agency (2019) <http://haberciniz.biz/depremin-merkez-ussu-golcuke-15-yil-sonra-yeni-lunapark-3113580h.htm>.
- Dolan, R., Fenster, M. S., & Holme, S. J. (1991). Temporal analysis of shoreline recession and accretion. *Journal of Coastal Research*, 7(3), 723–744. <https://www.jstor.org/stable/4297888>.
- Fereydooni, H., & Mojeddifar, S. (2017). A directed matched filtering algorithm (DMF) for discriminating hydrothermal alteration zones using the ASTER remote sensing data. *International Journal of Applied Earth Observation and Geoinformation*, 61, 1–13. <https://doi.org/10.1016/j.jag.2017.04.010>.
- Ferreira, M. P., Wagner, F. H., Aragao, L. E. O. C., Shimabukuro, Y. E., & Souza Filho, C. R. (2019). Tree species classification in tropical forests using visible to shortwave infrared WorldView-3 images and texture analysis. *ISPRS Journal of Photogrammetry and Remote Sensing*, 149, 119–131. <https://doi.org/10.1016/j.isprsjprs.2019.01.019>.
- Genz, A. S., Fletcher, C. H., Dunn, R. A., Frazer, L. N., & Rooney, J. J. (2007). The predictive accuracy of shoreline change rate methods and alongshore beach variation on Maui, Hawaii. *Journal of Coastal Research*, 23(1), 87–105. <https://doi.org/10.2112/05-0521.1>.
- Gibeaut, J. C., Hepner, T., Waldinger, R., Andrews, J., Gutierrez, R., Tremblay, T. A., Smyth, R., ve Xu, L. (2001). Changes in Gulf shoreline position, Mustang, and North Padre Islands, Texas. A Report of the Texas Coastal Coordination Council Pursuant to National Oceanic and Atmospheric Administration Award No. NA97OZ0179, GLO Contract Number 00-002R. The University of Texas at Austin, Austin, Texas, USA.
- Göney, S. (1963). İzmit Körfezi Kuzey Kıyılarıнын Jeomorfolojisi. *Türk Coğrafya Dergisi*, 22, 187–204.
- Güneroğlu, A. (2015). Coastal changes and land use alteration on northeastern part of Turkey. *Ocean & Coastal Management*, 118, 225–233. <https://doi.org/10.1016/j.ocecoaman.2015.06.019>.
- Himmelstoss EA, Farris AS, Henderson RE, Kratzmann MG, Ergul, Ayhan, Zhang, Ouya, Zichichi JL, Thieler ER (2018) Digital Shoreline Analysis System (version 5.0): U.S. Geological Survey software. <https://code.usgs.gov/cch/dsas/>.
- Hoşgören, M. Y. (1995). İzmit Körfezi Havzasının Jeomorfolojisi, İzmit Körfezi Kuvaterner İstifi. Editör, Meriç, E, 343–348.
- Kahya, O., (2005). Landsat Etm Verisi Kullanılarak Arazi Örtüsünün Expert Sistem Yöntemiyle Sınıflandırılması. Yıldız Teknik Üniversitesi Fen Bilimleri Enstitüsü, Yüksek Lisans Tezi.
- Kalkan, K., Maktav, D., Mercan O.Y., (2010). Kıyı Çizgisinin Otomatik Olarak Belirlenmesi ve Coğrafi Bilgi Sistemleri ile Entegrasyonu (Matlab Uygulaması). III. Uzaktan Algılama ve Coğrafi Bilgi Sistemleri Sempozyumu, 11–13 Ekim.
- Kuleli, T., Güneroğlu, A., Karlı, F., & Dihkan, M. (2011). Automatic detection of shoreline change on coastal Ramsar

- wetlands of Turkey. *Ocean Engineering*, 38(10), 1141–1149. <https://doi.org/10.1016/j.oceaneng.2011.05.006>.
- Lixin, G., Weixin, X., & Jihong, P. (2015). Segmented minimum noise fraction transformation for efficient feature extraction of hyperspectral images. *Pattern Recognition*, 48, 3216–3226. <https://doi.org/10.1016/j.patcog.2015.04.013>.
- Maiti, S., & Bhattacharya, A. (2009). Shoreline change analysis and its application to prediction: A remote sensing and statistics based approach. *Marine Geology*, 257, 11–23. <https://doi.org/10.1016/j.margeo.2008.10.006>.
- Mukhopadhyay, A., Mukherjee, S., Mukherjee, S., Ghosh, S., Hazra, S., & Mitra, D. (2012). Automatic shoreline detection and future prediction: A case study on Puri Coast, Bay of Bengal, India. *European Journal of Remote Sensing*, 45(1), 201–213. <https://doi.org/10.5721/EuJRS20124519>.
- Nassar, K., Mahmud, W. E., Fath, H., Masria, A., Nadaoka, K., & Negm, A. (2019). Shoreline change detection using DSAS technique: Case of North Sinai coast, Egypt. *Marine Georesources & Geotechnology*, 37(1), 81–95. <https://doi.org/10.1080/1064119X.2018.1448912>.
- Oyedotun TDT (2014) Shoreline geometry: DSAS as a tool for historical trend analysis. *Geomorphological Techniques*.
- Özmen B (2000) 17 Ağustos 1999 İzmit Körfezi Depremi'nin Hasar Durumu (Rakamsal Verilerle). TURKISH EARTHQUAKE FOUNDATION.
- Sheik, M., & Chandrasekar. (2011). A shoreline change analysis along the coast between Kanyakumari and Tuticorin, India, using digital shoreline analysis system. *Geo-spatial Information Science*, 14(4), 282–293. <https://doi.org/10.1007/s11806-011-0551-7>.
- Tağıl, Ş., & Cürebal, İ. (2005). Altnova (Balıkesir) Sahilinde Kıyı Çizgisi Değişimini Belirlemede Uzaktan Algılama ve Coğrafi Bilgi Sistemleri. *Fırat Üniv. Sosyal Bilimler Dergisi*, 15(2), 51–68 <https://hdl.handle.net/20.500.12462/5201>.
- Thang, N. T. X., Thu, T. V., ve Woodroffe, C. D., (2017) Coastal erosion vulnerability of Kien Giang - the Western Mekong River Delta Coast in Vietnam. International Conference on Globalisation, Climate Change and Sustainable Development, 26–28 April, Hatinh University.
- Uzun, M., ve Garipağaoğlu N. (2014) Kıyı Çizgisi Değişimin Yaratacağı Riskler Açısından İzmit Körfezi Kıyılarının Değerlendirilmesi. *Uluslararası Sosyal Araştırmalar Dergisi*, 7 (31), 469–480.
- Uzun, M. (2014). Hersek Deltasında (Yalova) Kıyı Çizgisi-Kıyı Alanı Değişimleri Ve Etkileri. *Doğu Coğrafya Dergisi*, 19(32), 24–48. <https://doi.org/10.17295/dcd.781>.
- Uzun, M. (2015). İzmit Körfezi Kıyılarında, Kıyı Jeomorfolojisi-Kıyı Kullanımı İlişkisinin Coğrafi Analizi. *Zeitschrift für die Welt der Türken / Journal of World of Turks*, 7(2), 351–375.
- Vatan Newspaper, (2015). <http://www.gazetevatan.com/yikintidan-filizlendi%2D%2D854757-yasam/>.
- Yunus Ali, P., & ve Narayana, A. C. (2015). Short-term morphological and shoreline changes at Trinkat Island, Andaman and Nicobar, India, after the 2004 tsunami. *Marine Geodesy*, 38(1), 26–39. <https://doi.org/10.1080/01490419.2014.908795>.

Publisher's note Springer Nature remains neutral with regard to jurisdictional claims in published maps and institutional affiliations.